The Aryl Hydrocarbon Receptor mediates reproductive toxicity of polychlorinated biphenyl congener 126 in rats

Violet Klenov,[1] Susanne Flor,[2] Shanthi Ganesan,[3] Malavika Adur[3], Nazmin Eti,[2] Khursheed Iqbal,[4] Michael J. Soares,[4,5,6] Gabriele Ludewig,[2] Jason W. Ross,[3] Larry W. Robertson,[2] and Aileen F. Keating[3,†]

[1]Dept of Ob/Gyn, University of Iowa, [2]Interdisciplinary Graduate Program in Human Toxicology and Dept of Occupational and Environmental Health, University of Iowa, [3]Dept of Animal Science, Iowa State University, [4]Institute for Reproduction and Perinatal Research and Department of Pathology, University of Kansas Medical Center, Kansas City, KS; [5]Departments of Pediatrics and Obstetrics and Gynecology, University of Kansas Medical Center, Kansas City, KS; [6]Center for Perinatal Research, Children's Research Institute, Children's Mercy, Kansas City, MO

[†] Corresponding author: akeating@iastate.edu

Study funding/competing interest(s): P42ES013661 to GL and LWR, ES029280 and ES028957 to MJS and the Iowa State University Bailey Career Development Award to AFK. The University of Virginia Center for Research in Reproduction Ligand Assay and Analysis Core is supported by the Eunice Kennedy Shriver NICHD/NIH Grant R24HD102061.

Abstract:

Polychlorinated biphenyls (PCBs) are endocrine disrupting chemicals with documented, though mechanistically ill-defined, reproductive toxicity. The toxicity of dioxin-like PCBs, such as PCB126, is mediated via the aryl hydrocarbon receptor (AHR) in non-ovarian tissues. The goal of this study was to examine the uterine and ovarian effects of PCB126 and test the hypothesis that the AHR is required for PCB126-induced reproductive toxicity. Female Holzman-Sprague Dawley wild type (n = 14; WT) and *Ahr* knock out (n = 11; $AHR^{-/-}$) rats received a single intraperitoneal injection of either corn oil vehicle (5 ml/kg: WT_O and $AHR^{-/-}$_O) or PCB126 (1.63 mg/kg in corn oil: WT_PCB and $AHR^{-/-}$_PCB) at four weeks of age. The estrous cycle was synchronized and ovary and uterus were collected 28 days after exposure. In WT rats, PCB126 exposure reduced ($P < 0.05$) body and ovary weight, uterine gland number, uterine area, progesterone, 17β-estradiol and anti-Müllerian hormone level, secondary and antral follicle and corpora lutea number but follicle stimulating hormone level increased ($P < 0.05$). In $AHR^{-/-}$ rats, PCB126 exposure increased ($P \leq 0.05$) circulating luteinizing hormone level. Ovarian or uterine mRNA abundance of biotransformation, and inflammation genes were altered ($P < 0.05$) in WT rats due to PCB126 exposure. In $AHR^{-/-}$ rats, the transcriptional effects of PCB126 were restricted to reductions ($P < 0.05$) in three inflammatory genes. These findings support a functional role for AHR in the female reproductive tract, illustrate AHR's requirement in PCB126-induced reprotoxicity, and highlight the potential risk of dioxin-like compounds on female reproduction.

Key words: Polychlorinated biphenyl, PCB126, reproductive toxicity, aryl hydrocarbon receptor, aryl hydrocarbon receptor knock out

Introduction:

Polychlorinated biphenyls (PCBs) are persistent organic pollutants that were extensively employed in the electrical, electronics, plastics, paint, and pesticide industries until production, but not use, was banned in the United States in 1977 due to harmful health effects [1]. Exposure to PCBs is ongoing, via ingestion of contaminated food, inhalation of contaminated air, and sometimes dermal/occupational exposure [2]. As a consequence, PCBs have been detected in the serum of 71% of reproductive aged women, as well as in human follicular fluid, ovarian tissue, placenta, uterine muscle, amniotic fluid, breast milk, semen, and fetal cord blood [3-5].

Polychlorinated biphenyls are endocrine disrupting chemicals broadly classified as dioxin-like and non-dioxin-like congeners based on their similarities in toxicity to 2,3,7,8-tetrachlorodibenzo-p-dioxin (TCDD) with PCB126 being the most potent dioxin-like toxin among PCBs [6]. Reproductive toxicity has been demonstrated in both animal and human studies following exposure to PCBs. In human women, PCB exposure has been associated with altered menstrual function, earlier onset of menopause, increased miscarriage risk, and increased time to pregnancy [5, 7-12]. In men, PCB exposure has been associated with decreased sperm parameters [5, 13] and endocrine disruption [14]. Furthermore, PCBs cross the placenta [15] and have transgenerational effects [16-19], including evidence of epigenetic alterations in sperm and brain [20]. Individuals exposed to PCBs *in utero* have decreased fecundity, reduced antral follicles, lower birth weight, and lower IQ [2, 21-24]. The mechanisms through which PCBs impart reproductive harm remain to be fully elucidated in both the male and the female, since both could contribute to reproductive and transgenerational impacts of PCBs.

Although PCB126 was a minor component of commercial PCB mixtures, it contributes a majority of dioxin equivalents in many environmental samples [25]. The half-life of PCB126 in humans is years in duration [26]. Many biologic effects of PCBs are receptor mediated and dioxin-like PCBs, including PCB126, bind to the aryl hydrocarbon receptor (AHR), a cytosolic, ligand–activated, nuclear transcription factor [27]. The most well studied AHR target genes include those of the cytochrome P450 family, such as *Cyp1a1*, *Cyp1a2* and *Cyp1b1*, which encode xenobiotic metabolizing enzymes [28]. Exposure to PCB126 increases transcript abundance of the *Cyp1* genes in rat liver, lung, spleen, kidney, stomach and thymus [29]. Biotransformation of endogenous and xenobiotic compounds can result in the formation of toxic metabolites as well as metabolic byproducts including reactive oxygen species. It is proposed that activation of the AHR and its downstream effects contribute to PCB-induced adverse health outcomes [30]. Furthermore, the AHR pathway interacts with the estrogen receptor pathway and multiple immunologic pathways, thus, AHR activation could be responsible for altered immunologic and endocrine phenotypes [31-34].

The AHR is highly conserved among mammalian species and is found throughout the reproductive tract, including in the uterus and ovaries of both animals and humans [28, 35]. Although AHR function after toxicant exposure has been investigated widely for the past 40 years, its physiological role has only recently been evaluated [32]. Understanding the role of AHR in reproductive biology is insufficient, though it is known that the absence of *Ahr* in mice leads to impaired reproductive function [28].

This study used a rat model of AHR deficiency to investigate whether adverse reproductive effects following PCB126 exposure are mediated by the AHR and to investigate ovarian PCB126 biotransformation and inflammation mRNA induction in the ovary and uterus.

Materials and Methods:

Aryl Hydrocarbon Knock Out rats

The AHR$^{-/-}$ rat model was developed at the University of Kansas Medical Center after obtaining approval from the Institutional Animal Care and Use Committee with a Holzman-Sprague Dawley rat strain. The model was generated using CRISPR/Cas9-mediated disruption of the *Ahr* basic helix loop helix DNA binding domain. *Ahr* mutant rats identical to those used in this experiment are available at the Rat Resource & Research Center (RRRC# 831; strain name SD-Ahrem1Soar; University of Missouri, Columbia, MO; www.rrrc.us).

Chemicals

PCB126 (3,3',4,4',5-pentachlorobiphenyl) was synthesized, purified, and characterized as described in previous publications from our group [36].

Experimental design

A total of 25 female rats, 14 wild type (WT) and 11 AHR$^{-/-}$, were included in the study. Rats were fed a standard rodent diet (Teklad 8604, Envigo), and singly housed in a wire cage with a controlled environment (14:10 h light:dark cycle). All animals had free access to food and water. Both WT and KO rats were injected with a single intraperitoneal (i.p.) dose of corn oil vehicle (5 mL/kg body weight) or PCB126 (1.63 mg/kg body weight), equivalent to 5 µmol/kg body weight) in corn oil at four weeks of age (experimental day one). This dose was chosen as it has been used in several earlier studies to investigate effects of PCB126 exposure while

minimizing overt toxicity [37, 38]. Since a major goal of the study was to identify a functional role for the AHR in modulating ovarian PCB126-induced effects, a PCB126 dose that is known to cause systemic toxicity was required. There was a total of four groups: WT_O (n = 7), WT_PCB (n = 7), $AHR^{-/-}$_O (n = 5) and $AHR^{-/-}$_PCB (n = 6). Two deaths occurred in the WT-PCB group following injection but prior to planned necropsy date. After 24 days of exposure, all rats received a one-time intraperitoneal injection of 40 µg gonadotropin releasing hormone (L4513, Sigma-Aldrich) dissolved in sterile phosphate buffered saline (PBS) to synchronize estrous cycles prior to euthanasia and all animals were confirmed to be at the estrus stage at euthanasia. Twenty-eight days following exposure to PCB126, rats were euthanized using carbon-dioxide asphyxiation followed by thoracotomy. After euthanasia, whole blood was collected through cardiac puncture into non-anticoagulant coated tubes. Blood was allowed to clot at room temperature and centrifuged at 1500 x g for 10 min. Serum was aliquoted from each animal and frozen at -80°C. Serum 17β-estradiol, progesterone, testosterone, follicle stimulating hormone (FSH), luteinizing hormone (LH) and anti-Müllerian hormone (AMH) were measured at the University of Virginia Center for Research in Reproduction Ligand Assay and Analysis Core (https://med.virginia.edu/research-in-reproduction/contact-us/ligand-assay-analysis-core/) with appropriate controls for each assay included. Vaginal smears were collected and analyzed according to previously published protocols [39, 40]. The ovaries and uteri were dissected, removed, and weighed. One ovary and one uterine horn per animal was fixed in 10% neutral buffered formalin and the other ovary and uterine horn were flash frozen in liquid nitrogen and stored at -80°C.

Ovarian Follicle Counting

Formalin fixed ovaries from five animals per treatment group (n = 20) were embedded in paraffin and serially sectioned at a thickness of 5 µm. Every 12th section was mounted on a microscope slide and stained with hematoxylin and eosin. Two blinded assessors performed independent follicle counts. Inter-assessor reliability was determined using the intraclass correlation coefficient (ICC) and means of values from the assessors were used in the analysis. Statistical analysis was performed using one-way ANOVA (SPSS 25).

Uterine Histological Evaluation

Formalin fixed uterine horns from all animals (n = 23) were embedded in paraffin. 5 µm thick sections were selected from each quarter of the specimen (four sections per horn/animal) to obtain representative images of the entire horn. Sections were mounted and stained with hematoxylin and eosin. Images were captured of each of the four sections per animal with the same microscope configuration and magnification. Images were then analyzed in a blinded fashion and total uterine area (number of endometrial glands and glands per unit area) was calculated. Image J software (NIH, https://imagej.nih.gov/ij/index.html) was used for the analysis with appropriate calibration.

Uterine Immunohistochemistry

A total of ten 5 µm thick tissue sections from each of the 23 animals were used to assess the relative expression of estrogen receptor alpha and estrogen receptor beta proteins in the uterus using immunohistochemistry. Sections were deparaffinized in Citrisolv^{TM} and rehydrated in graded ethanol. Antigen retrieval was performed by microwaving sections in sodium citrate buffer at full power for 10 minutes (10 mM sodium citrate, pH 6 with 0.5% Tween). Sections

were cooled to room temperature and incubated in a solution containing 5% goat serum, 1% bovine serum albumin, 1% DMSO and Image IT-Fx (I36933, ThermoFisher) in PBS for one hour at room temperature to block nonspecific binding. The sections were incubated overnight at 4°C with either rabbit monoclonal antibody against estrogen receptor alpha (ERA) (1:100, ab32063, Abcam), rabbit polyclonal antibody against estrogen receptor beta (ERB) (1:100, ab3576, Abcam) or no primary antibody (negative control). After primary antibody binding, the sections were washed in PBS and incubated with Alexa-Fluor 488 conjugated goat anti-rabbit (1:200, 4412S, Cell Signaling) secondary antibody for 90 minutes at room temperature in a humidified slide incubation chamber. Sections were washed in PBS and mounted using SlowFade^{TM} Gold mountant containing 4′,6-diamidino-2-phenylindole (DAPI) for counterstaining (S36938, ThermoFisher). All images were captured with a Leica DMI3000 B fluorescence microscope at the same intensity, exposure, and magnification.

Evaluation of immunohistochemical data

The quantification of estrogen receptor expression in the uterus was performed in three compartments: the stroma, luminal epithelium, and glandular epithelium. Of the ten tissue sections per animal, five were used to investigate the ERA and the other five were used to investigate the ERB. One of those five was used as a negative control for each antibody per animal. Acquired microscope images had adequate representation of all compartments of interest. Two images were taken of each primary antibody-stained section and one image was captured of the negative controls. ImageJ software was then used in a blinded fashion to calculate the total immunofluorescence in each compartment of interest in each image. Acquisition settings remained stable for each image.

RNA isolation, reverse transcription, and RT^2 profiler PCR arrays

Ribonucleic acid (RNA) was isolated from ovaries and uteri to perform RT^2 profiler PCR arrays. Two different arrays, the rat metabolism array (PARN-002Z, Qiagen) and rat inflammation array (PARN-011Z, Qiagen), were employed on ovarian tissue. Ovarian RNA from three animals per exposure group was included in each array (n = 12). The same rat inflammation array was used on uterine tissue, also including RNA from three animals per exposure group (n = 12).

RNA was isolated using RNeasy Mini kit (Qiagen) and concentrations determined using a ND-1000 Spectrophotometer (λ = 260/280 nm; NanoDrop Technologies). Total RNA (200 ng) was reverse transcribed to complementary DNA (cDNA) using an RT^2 first-strand kit (Qiagen) combined with an appropriate RT^2 SYBR Green master mix (Qiagen). The regular cycling program consisted of a 10 min hold at 95°C and 40 cycles of denaturing at 95°C for 15 sec along with a combined annealing and extension for 1 min at 60°C. Data were normalized with *Actb*, *B2m*, *Hprt1*, *Ldha*, and *Rplp1* housekeeping genes and analyzed using Qiagen software (https://www.qiagen.com/us/shop/genes-and-pathways/data-analysis-center-overview-page/). All appropriate technical controls were employed, including no template and no primer controls. A fold change cut off of two was used.

Statistical analysis

For all experiments, statistical analysis was performed using two-way ANOVA (SPSS 25) with post-hoc t-test with Welch's correction. A biologically meaningful change was considered if the *P*-value was ≤ 0.05.

Results

Impact of AHR deficiency and PCB126 exposure on body, ovarian and uterine weight.

There was no difference in mean body weight between the groups at the beginning of the experimental period. After 28 days of exposure to PCB126, rats in the WT_PCB group weighed less than WT_O rats ($P < 0.05$), whereas there was no difference between the $AHR^{-/-}$_O and $AHR^{-/-}$_PCB groups ($P > 0.05$; Figure 1A). There was also no difference in body weight between the WT_O and $AHR^{-/-}$_O groups ($P > 0.05$; Figure 1A). Relative ovarian weight (ovarian weight/body weight) was reduced in the WT_PCB group compared to WT_O ($P < 0.05$), whereas there was no difference between $AHR^{-/-}$_O and $AHR^{-/-}$_PCB ($P > 0.05$) or between WT_O and $AHR^{-/-}$_O rats ($P > 0.05$) (Figure 1B). Relative uterine weight did not differ between any groups ($P > 0.05$; Figure 1C).

Effect of AHR loss and PCB126 exposure on circulating hormones

Exposure to PCB126 in WT rats increased ($P < 0.05$) FSH and decreased ($P < 0.05$) progesterone, 17β-estradiol, and AMH level (Figure 2). There was no difference ($P > 0.05$) between treatment groups in serum levels of testosterone (Figure 2D). Luteinizing hormone was higher in the $AHR^{-/-}$_PCB than in $AHR^{-/-}$_O ($P = 0.05$) rats (Figure 2B). AHR deficiency reduced ($P < 0.05$) circulating AMH level relative to WT_O rats (Figure 2F).

Impact of AHR deficiency and PCB126 exposure on ovarian follicle composition

There was no difference ($P > 0.05$) in the mean number of primordial or primary follicles between any groups (Figure 3A,B). In WT rats, exposure to PCB126 reduced ($P < 0.05$) secondary (Figure 3C), antral (Figure 3D) follicle and corpora lutea (Figure 3E) number. In $AHR^{-/-}$ rats, there was no effect of PCB126 exposure on any follicle stage ($P > 0.05$; Figure 3A-D). There was also no difference in number of follicles of corpora lutea between WT_O and $AHR^{-/-}$_O ovaries.

Uterine impacts of AHR deficit and PCB126 exposure

Mean uterine area was reduced ($P < 0.05$) in the WT_PCB compared to the WT_O rats, whereas there was no difference ($P > 0.05$) between the $AHR^{-/-}$_O and $AHR^{-/-}$_PCB rats (Figure 4A). There was also no difference ($P > 0.05$) in uterine area between the WT_O and $AHR^{-/-}$_O groups (Figure 4A). Mean uterine gland number was reduced ($P < 0.05$) in the WT_PCB group as compared to the WT_O group, whereas there was no difference ($P > 0.05$) between the $AHR^{-/-}$_O and $AHR^{-/-}$_PCB rats (Figure 4B). There was no difference ($P > 0.05$) in uterine gland number between the WT_O and $AHR^{-/-}$_O rats (Figure 4B). Neither PCB126 exposure nor AHR deficiency affected the ratio of glands/μm^2 area (Figure 4C).

Effect of AHR loss or PCB126 exposure on uterine abundance of estrogen receptors.

There was no difference ($P > 0.05$) in abundance of the ERA (Figure 5A) or the ERB (Figure 5B) protein in any of the uterine compartments analyzed (stroma, luminal epithelium, and glandular epithelium) due to PCB126 exposure. Loss of AHR reduced ERA levels in the stroma ($P < 0.05$; Figure 5A) and the GE ($P < 0.05$; Figure 5A) but there was no impact of AHR

loss on ERA abundance in the LE (Figure 5A), nor was there any impact of AHR deficiency on ERB straining in any compartment (Figure 5B).

Effect of PCB126 exposure on ovarian and uterine mRNA abundance

Ovarian chemical biotransformation mRNA effects

Exposure to PCB126 altered the abundance ($P < 0.05$) of mRNA encoding 46 of the 84 chemical metabolism genes analyzed in WT rats (WT_O v WT_PCB; Table 1). Similarly, the abundance of mRNA encoding 31 genes were altered ($P < 0.05$) due to loss of AHR (WT_O vs. $AHR^{-/-}$_O; Table 2). However, there were no PCB126-induced alterations observed in the mRNA level of any genes in the $AHR^{-/-}$ rats (AHR_O v AHR_PCB).

Ovarian inflammation mRNA impacts

Ten genes differed ($P < 0.05$) due to PCB126 exposure in the WT rats (WT_O v WT_PCB; Table 3), while only three were altered ($P < 0.05$) in the $AHR^{-/-}$ rats due to PCB126 exposure ($AHR^{-/-}$_O vs. $AHR^{-/-}$_PCB; Table 4). Three genes ($P < 0.05$) were reduced in abundance in $AHR^{-/-}$_O relative to WT_O rats (WT_O vs. $AHR^{-/-}$_O; Table 5).

Uterine inflammation mRNA impacts

Exposure to PCB126 altered ($P < 0.05$) uterine mRNA encoding 13 genes in WT rats (WT_O v WT_PCB; Table 6), while there were no impacts ($P > 0.05$) on abundance of mRNA encoding investigated genes in the $AHR^{-/-}$ rats exposed to PCB126 ($AHR^{-/-}$_O vs. $AHR^{-/-}$_PCB). One gene differed ($P < 0.05$) in transcript abundance between the WT_O and the $AHR^{-/-}$–O (Table 7).

Discussion

While production of PCBs has been banned worldwide, humans continue to be exposed to these compounds due to their persistent nature. Reproductive aged women in the United States currently have detectable levels of PCBs in their serum [3, 4]. There is sufficient evidence to suggest that PCB exposure leads to adverse reproductive outcomes [41-43] and potentially even inter- [16] and trans-generational damage [17]. Endocrine disruption [18] and altered hypothalamic gene expression [19] across generations due to Aroclor 1221 exposure have been determined in rats. In the ovary, PCB126 exposure decreased follicle number, reduced 17ß-estradiol and progesterone, and altered estrous cyclicity in exposed rats [44]. PCB126 exposure also decreased progesterone synthesis [45], and decreased 17β-estradiol [46] in cultured porcine luteal cells. In cultured bovine luteal cells PCB126 reduced calcium mobilization in granulosa cells, potentially affecting ovarian steroidogenesis [47]. Further evidence for an ovarian impact of PCB126 exposure due to induction of mitochondrial apoptotic pathway has been demonstrated [48]. Despite these studies, modes of ovarian action of PCB126 remain unclear.

The aims of this study were two-fold: the first was to determine ovarian and uterine effects of PCB126 and to determine if the ovary has the xenobiotic biotransformation capacity to respond to PCB126 exposure and the second was to use a rat model of AHR deficiency to investigate the requirement and involvement of AHR in PCB126-induced ovarian and uterine dysfunction. Transgenic rodent models have been used to investigate the role of the AHR in reproductive organ development and function. Mice deficient in AHR had reductions in ovarian reserve, reduced 17β-estradiol production, altered uterine 17β-estradiol response, and increased

rates of miscarriage [28, 49]. No studies on female reproductive function have been performed in AHR deficient rats, nor are there any studies in rats and mice assessing the AHR response to PCB126 exposure in the ovary or uterus. For this reason, the dose chosen for the study was one that is known to cause PCB126-induced toxicity but which does not cause overt systemic toxicity as evidenced by a recent study in which body weight gain was unaffected by PCB126 exposure for approximately 35 days after exposure [6]. In order to assess if AHR deficiency affected PCB126-induced female reproductive toxicity, a dose that caused effects in the WT rats was required. The half-life of PCB126 in humans is 3.32-5.58 years with the fat composition of the body influencing the elimination time [26]. In rats, PCB126 was determined not to have declined over a 22-day period, indicating a slow elimination [50]. Thus, in this study, a single dose of PCB126 at a dose known to cause toxicity was utilized to assess both basal reproductive toxicity as well as to determine a role for the AHR in mediating these effects.

At the onset of dosing there was no difference in body weight across the experimental groups. It is noteworthy that two rats in the WT group who were exposed to PCB died, though no $AHR^{-/-}$ rats had this response. In addition, WT rats lost body weight post PCB126 exposure, but the $AHR^{-/-}$ rats displayed no effect of PCB126 exposure on their body weight. These findings imply a systemic impact of PCB126 exposure in the WT but not the $AHR^{-/-}$ rats. The PCB126-induced decline in body weight was unexpected and could have resulted in PCB-induced secondary effects that altered ovarian and uterine function. This is an area for future research on PCB126-induced reproductive toxicity.

The ovary weight was lower in the WT but not AHR$^{-/-}$ rats, suggesting that ovotoxicity occurred due to PCB126 exposure. Follicle depletion can result from toxicant exposure [51] and there were decreased numbers of secondary and antral follicles in the WT rats exposed to PCB126. This follicle depleting impact of PCB126 exposure was limited to the large pre-antral and antral follicles, since there was no impact of PCB126 exposure on primordial or small follicle number. These findings were in agreement with a previous study on PCB126 exposed rats in which antral follicles were reduced in number, however that study classified ovarian follicles only as pre-antral or antral [44], thus the current study has determined that PCB126-induced follicle loss is evident at the secondary follicle stage onwards. The AHR$^{-/-}$ rats treated with either oil or PCB126 did not differ from the WT control rats in any follicle stage of development. Loss of more developed follicles induced by PCB126 in WT rats could be phenotypically manifested as anovulation or lowered 17β-estradiol levels in circulation. These findings support a specificity for PCB126 on reducing secondary and antral follicles but not more immature follicles stages and also provide evidence that the AHR is required for ovarian toxicity that occurs due to PCB126 exposure.

The ovary is a steroidogenic organ and ovaries were collected at estrus, at which time 17β-estradiol is the predominant sex steroid hormone present. Exposure to PCB126 exposure reduced circulating 17β-estradiol and progesterone and increased follicle stimulating hormone. The reduction in 17β-estradiol and progesterone is in alignment with reduced levels of antral follicles and corpora lutea in the ovary due to PCB126 exposure. A recent study determined increased *Cyp17a1* and *Cyp19a1* transcript abundance and increased intra-ovarian 17β-estradiol content in *Ahr*$^{-/-}$ adult mice relative to their WT littermates [52]. In addition, increased follicle

stimulating hormone as noted herein could result from decreased 17β-estradiol and is often a clinical indicator of ovarian senescence [53]. Exposure to PCB126 increased LH in the $AHR^{-/-}$ rats but not the WT rats, potentially indicating a direct pituitary effect of PCB126 exposure in the absence of AHR. No impact of AHR deficiency was noted on LH level, however, LH was lower in pre-pubertal *Ahr*$^{-/-}$ mice, relative to their WT counterparts, but this was not sustained into adulthood [52]. In addition, PCB126 exposure decreased the abundance of circulating anti-Müllerian hormone in WT rats, which is likely a secondary effect of the observed reduction in secondary and antral follicle number caused by PCB126 exposure since anti-Müllerian hormone is produced by those follicle stages. This PCB126-reduced anti-Müllerian hormone was not observed in the $AHR^{-/-}$ rats, indicating that PCB126 is an ovarian endocrine disruptor and that this is mediated through the AHR.

In WT rats exposed to PCB126, there were increases in 44 and decreases in two ovarian mRNA transcript levels, indicating that the ovary responded to the PCB126 exposure in chemical metabolism gene induction. Many of these genes, including *Cyp1a1, Cyp1b1* and *Gstp1* are known targets of the AHR [54-56], thus our findings recapitulated what is known about AHR function. These data do not discount a functional role for additional transcription factors in regulating transcription of the genes investigated. Interestingly in WT rats, *Ahr* mRNA was also induced, which indicates that *Ahr* is important for the ovarian response to PCB126 exposure recapitulating previous findings [57]. Both *Gpx1* and *Ggt1* were reduced by PCB126 exposure in the ovary. Interestingly, Gpx1 was also reduced in livers of PCB exposed male rats [38]. The ovarian involvement of *Gpx1* as an antioxidant has been documented in response to other ovotoxicants [58-60] and to be altered with ovarian aging [61]. Less is known regarding the

ovarian role of *Ggt1*, though an association with GGT1 abundance and incidence of ovarian tumors [62] and *Ggt1* polymorphism and polycystic ovarian syndrome is documented [63].

Exposure to PCB126 increased mRNA encoding paraoxonase 1 (*Pon1*) which we previously observed to be also increased by PCB126 exposure in rat livers [64]. The PON1 enzyme activity in follicular fluid was associated with serum levels [65] and it was proposed that PON1 protein was transported into the follicle by HDL. Also, *Pon1* polymorphism is associated with increased risk for polycystic ovarian syndrome [66]. Myeloperoxidase 1 (*Mpo1*), an oxidant generating enzyme, was increased in the ovary of WT rats exposed to PCB126. While normally expressed only in myeloid cells, aberrant MPO expression has been observed in other tissues and associated with various diseases. Atypical MPO levels can lead to oxidative damage and elevated MPO was associated with ovarian cancer potentially through reduced apoptosis in epithelial ovarian cancers [67]. Additional genes that are known to have important functional roles in the ovary were increased in abundance in the WT PCB126-exposed rats include *Cyp17a1*, *Hsb17b3* and *Cyp19a1* which are involved in the production of 17β-estradiol in the steroidogenic pre-ovulatory follicles. Despite reduced circulating 17β-estradiol, the ovary may be compensating to induce steroidogenic gene mRNA abundance. Thus, in the WT rats, exposure to PCB126 induced genes involved in chemical biotransformation and steroidogenesis. In the rats deficient in AHR, there was a complete absence of any changes in mRNA transcript abundance, supporting an important functional role for AHR in PCB126 ovarian biotransformation.

It is recognized that PCB126 exposure has immunological effects [68-70], thus, the study determined if there were alterations in mRNAs of genes encoding inflammatory proteins in both

the ovary and the uterus. In the ovary of WT rats, PCB126 exposure increased the abundance of 10 inflammatory mRNAs including the tumor necrosis factor family members, *Tnfsrsf11b* and *Tnfsf10*. As the receptor for RANKL, increased *Tnfsrsf11b* could indicate altered granulosa cell communication [71]. *Tnfsf10 (Trail*) induces ovarian apoptosis [72] and is increased in ovaries from females with metabolic disease [73] suggesting involvement in cell death responsible for the observed lower follicle number in the PCB126 exposed rats. In aging ovaries, IL6 has been determined to be reduced [74], potentially indicating a role for PCB126-induced *Il6st* in a pro-apoptotic function in this study. Corresponding also to the PCB126-reduced follicle numbers were increased *Bmp2* as potentially a compensatory response since BMP2 has roles in folliculogenesis [75] and viability of secondary follicles [76]. The chemokine receptor, *Ccr1*, was increased by PCB126 exposure, and has an ovarian role [77] and is observed to be involved in ovarian inflammation as a receptor for CCL5 [78]. Other biomarkers for polycystic ovary syndrome, *Csf1* [79] and *Pf4* [80] were increased by PCB126 exposure. The receptor for IL1 was increased by PCB126 exposure and Il1 deficiency is associated with a prolonged ovarian lifespan [81]. The *Cxc3cr1* gene encodes the receptor for fractalkine which has a role in regulation of ovarian steroidogenesis in LH-responsive granulosa cells [82] and in modulating PI3K signaling [83], a known folliculogenesis regulator [84]. In the rats deficient in the AHR, there were decreased abundance of three mRNAs, *Ccl11*, *Ccl22* and *Il11* due to PCB126 exposure. Increased ovarian stromal expression of *Ccl11* is associated with ovarian aging [85], Il11 is increased in ovulatory follicles in the rat ovary [86] while less regarding a role for ovarian Ccl22 is known. Thus, these mRNAs could be direct targets of PCB126 independent of the AHR. Taken together, exposure to PCB126 in WT rats induced mRNAs related to apoptosis,

steroidogenesis regulation and with roles in ovarian pathologies, supporting an ovarian dysfunction-induction by PCB126 exposure.

Uterine gland number and uterine area were both reduced in response to PCB126 exposure, but this effect was absent in the AHR deficient rats. A negative impact of PCB126 on uterine weight was previously reported [87], however our study was at a lower PCB126 exposure and this was not noted herein. The impact of PCB126 exposure on uterine inflammatory mRNAs as well as the localization and abundance of the estrogen receptors were investigated. Thirteen uterine mRNAs were altered by PCB126 exposure in WT rats with only one of these being reduced in abundance. Three mRNAs with roles in uterine endometrial function, *Ccl24* [88, 89], *Ccl19* [90], *Ccl5* [91, 92], were increased by PCB126 exposure. Increased *Il33* observed due to PCB126 exposure is associated with inflammation during endometriosis [93] as is abnormal expression of *Il1r1* [94] and *Ccr1* [95]. Uterine BMP2 is a marker of decidualization [96] and was increased by PCB126 exposure. Increased *Pf4* is associated with endometrial cancer [97] and endometritis [98]. Less is known about the uterine function of *Tnfrsf11b* though lack of the ligand, RANKL, in mice is associated with higher pre-term fetal loss [99]. Uterine roles for *Cx3cr1*, *Cxcl12* and *Cxcr5* are documented related to maternal-conceptus interface [100, 101], endometriosis [102] and endometrial remodeling [103]. Another gene with a role in endometriosis, Ldha [104], had reduced abundance due to PCB126 exposure. In the AHR deficient rats, increased *Il2rb* was noted, potentially an AHR-independent target of PCB126. A role for *Il2rb* in endometrial hyperplasia is supported in mice [105]. Despite reduced 17β-estradiol in PCB126 exposure WT rats, no impact of PCB126 exposure was observed on the level of ERA and ERB in stroma, luminal or glandular epithelium in either the WT or AHR

deficient rats, discounting this as a PCB126 mode of action. Interestingly, lack of AHR reduced levels of ERA but not ERB in the stroma and glandular epithelium in the absence of a PCB126 exposure. Collectively, these findings support that there are PCB126-induced alterations to genes with roles in uterine pathology including endometriosis in agreement with recent human studies associating PCB exposure with increased risk for this disease [106].

This study supports activation of the AHR by PCB126, and that the ovary responds to PCB126 exposure in the form of increased xenobiotic metabolism and inflammatory mRNAs. Further, as summarized in Figure 6, in WT rats, PCB126 exposure reduces body weight, ovary weight, secondary and antral follicles, corpora lutea, progesterone, 17β-estradiol, AMH, uterine gland number and area, increased FSH, and alters ovarian chemical biotransformation and inflammatory mRNA levels. These responses were almost completely absent in rats deficient in AHR, demonstrating the requirement for AHR action for ovarian and uterine impacts of PCB126. Although ovarian steroid hormones were not affected by PCB126 exposure in $AHR^{-/-}$ rats, LH was increased. Thus, PCB126 acts as an endocrine disruptor with strong evidence of a role for the AHR in this outcome. The impact of PCB126 on several hormones could be a secondary effect of the reduction in large pre-ovulatory follicles, altered systemic metabolism or changes to hormone half-life. Several of the mRNAs identified to be altered in the ovary and uterus by PCB126 exposure are associated with polycystic ovary syndrome and endometriosis, respectively, two common reproductive pathologies that affect a large number of women.

References cited:

1. Faroon OM, Keith S, Jones D, de Rosa C. Effects of polychlorinated biphenyls on development and reproduction. Toxicol Ind Health 2001; 17:63-93.

2. Kristensen SL, Ramlau-Hansen CH, Ernst E, Olsen SF, Bonde JP, Vested A, Halldorsson TI, Rantakokko P, Kiviranta H, Toft G. Prenatal exposure to persistent organochlorine pollutants and female reproductive function in young adulthood. Environ Int 2016; 92-93:366-372.
3. Meeker JD, Maity A, Missmer SA, Williams PL, Mahalingaiah S, Ehrlich S, Berry KF, Altshul L, Perry MJ, Cramer DW, Hauser R. Serum concentrations of polychlorinated biphenyls in relation to in vitro fertilization outcomes. Environ Health Perspect 2011; 119:1010-1016.
4. Axelrad DA, Goodman S, Woodruff TJ. PCB body burdens in US women of childbearing age 2001-2002: An evaluation of alternate summary metrics of NHANES data. Environ Res 2009; 109:368-378.
5. Dallinga JW, Moonen EJ, Dumoulin JC, Evers JL, Geraedts JP, Kleinjans JC. Decreased human semen quality and organochlorine compounds in blood. Hum Reprod 2002; 17:1973-1979.
6. Gadupudi GS, Klaren WD, Olivier AK, Klingelhutz AJ, Robertson LW. PCB126-Induced Disruption in Gluconeogenesis and Fatty Acid Oxidation Precedes Fatty Liver in Male Rats. Toxicol Sci 2016; 149:98-110.
7. Axmon A, Rylander L, Stromberg U, Hagmar L. Altered menstrual cycles in women with a high dietary intake of persistent organochlorine compounds. Chemosphere 2004; 56:813-819.
8. Mendola P, Buck GM, Sever LE, Zielezny M, Vena JE. Consumption of PCB-contaminated freshwater fish and shortened menstrual cycle length. Am J Epidemiol 1997; 146:955-960.
9. Grindler NM, Allsworth JE, Macones GA, Kannan K, Roehl KA, Cooper AR. Persistent organic pollutants and early menopause in u.s. Women. PLoS One 2015; 10:e0116057.
10. Toft G, Thulstrup AM, Jonsson BA, Pedersen HS, Ludwicki JK, Zvezday V, Bonde JP. Fetal loss and maternal serum levels of 2,2',4,4',5,5'-hexachlorbiphenyl (CB-153) and 1,1-dichloro-2,2-bis(p-chlorophenyl)ethylene (p,p'-DDE) exposure: a cohort study in Greenland and two European populations. Environ Health 2010; 9:22.
11. Buck Louis GM, Dmochowski J, Lynch C, Kostyniak P, McGuinness BM, Vena JE. Polychlorinated biphenyl serum concentrations, lifestyle and time-to-pregnancy. Hum Reprod 2009; 24:451-458.
12. Buck Louis GM, Sundaram R, Schisterman EF, Sweeney AM, Lynch CD, Gore-Langton RE, Maisog J, Kim S, Chen Z, Barr DB. Persistent environmental pollutants and couple fecundity: the LIFE study. Environ Health Perspect 2013; 121:231-236.
13. Paul R, Moltó J, Ortuño N, Romero A, Bezos C, Aizpurua J, Gómez-Torres MJ. Relationship between serum dioxin-like polychlorinated biphenyls and post-testicular maturation in human sperm. Reprod Toxicol 2017; 73:312-321.
14. Petersen MS, Halling J, Jørgensen N, Nielsen F, Grandjean P, Jensen TK, Weihe P. Reproductive Function in a Population of Young Faroese Men with Elevated Exposure to Polychlorinated Biphenyls (PCBs) and Perfluorinated Alkylate Substances (PFAS). Int J Environ Res Public Health 2018; 15.

15. Mori C, Nakamura N, Todaka E, Fujisaki T, Matsuno Y, Nakaoka H, Hanazato M. Correlation between human maternal-fetal placental transfer and molecular weight of PCB and dioxin congeners/isomers. Chemosphere 2014; 114:262-267.
16. Pocar P, Fiandanese N, Secchi C, Berrini A, Fischer B, Schmidt JS, Schaedlich K, Rhind SM, Zhang Z, Borromeo V. Effects of polychlorinated biphenyls in CD-1 mice: reproductive toxicity and intergenerational transmission. Toxicol Sci 2012; 126:213-226.
17. Sakurada Y, Shirota M, Mukai M, Inoue K, Akahori F, Watanabe G, Taya K, Shirota K. Effects of vertically transferred 3,3',4,4',5-pentachlorobiphenyl on gene expression in the ovaries of immature Sprague-Dawley rats. J Reprod Dev 2007; 53:937-943.
18. Mennigen JA, Thompson LM, Bell M, Tellez Santos M, Gore AC. Transgenerational effects of polychlorinated biphenyls: 1. Development and physiology across 3 generations of rats. Environ Health 2018; 17:18.
19. Gore AC, Thompson LM, Bell M, Mennigen JA. Transgenerational effects of polychlorinated biphenyls: 2. Hypothalamic gene expression in rats. Biol Reprod 2021.
20. Gillette R, Son MJ, Ton L, Gore AC, Crews D. Passing experiences on to future generations: endocrine disruptors and transgenerational inheritance of epimutations in brain and sperm. Epigenetics 2018; 13:1106-1126.
21. Papadopoulou E, Caspersen IH, Kvalem HE, Knutsen HK, Duarte-Salles T, Alexander J, Meltzer HM, Kogevinas M, Brantsaeter AL, Haugen M. Maternal dietary intake of dioxins and polychlorinated biphenyls and birth size in the Norwegian Mother and Child Cohort Study (MoBa). Environ Int 2013; 60:209-216.
22. Fein GG, Jacobson JL, Jacobson SW, Schwartz PM, Dowler JK. Prenatal exposure to polychlorinated biphenyls: effects on birth size and gestational age. J Pediatr 1984; 105:315-320.
23. Caspersen IH, Haugen M, Schjolberg S, Vejrup K, Knutsen HK, Brantsaeter AL, Meltzer HM, Alexander J, Magnus P, Kvalem HE. Maternal dietary exposure to dioxins and polychlorinated biphenyls (PCBs) is associated with language delay in 3year old Norwegian children. Environ Int 2016; 91:180-187.
24. Jacobson JL, Jacobson SW. Intellectual impairment in children exposed to polychlorinated biphenyls in utero. N Engl J Med 1996; 335:783-789.
25. Iwata H, Watanabe M, Okajima Y, Tanabe S, Amano M, Miyazaki N, Petrov EA. Toxicokinetics of PCDD, PCDF, and coplanar PCB congeners in Baikal seals, Pusa sibirica: age-related accumulation, maternal transfer, and hepatic sequestration. Environ Sci Technol 2004; 38:3505-3513.
26. Gao Q, Ben Y, Dong Z, Hu J. Age-dependent human elimination half-lives of dioxin-like polychlorinated biphenyls derived from biomonitoring data in the general population. Chemosphere 2019; 222:541-548.
27. Haarmann-Stemmann T, Abel J. The arylhydrocarbon receptor repressor (AhRR): structure, expression, and function. Biol Chem 2006; 387:1195-1199.
28. Hernandez-Ochoa I, Karman BN, Flaws JA. The role of the aryl hydrocarbon receptor in the female reproductive system. Biochem Pharmacol 2009; 77:547-559.
29. Wang B, Robertson LW, Wang K, Ludewig G. Species difference in the regulation of cytochrome P450 2S1: lack of induction in rats by the aryl hydrocarbon receptor agonist PCB126. Xenobiotica 2011; 41:1031-1043.

30. Pocar P, Brevini TA, Fischer B, Gandolfi F. The impact of endocrine disruptors on oocyte competence. Reproduction 2003; 125:313-325.
31. Stockinger B, Di Meglio P, Gialitakis M, Duarte JH. The aryl hydrocarbon receptor: multitasking in the immune system. Annu Rev Immunol 2014; 32:403-432.
32. Beischlag TV, Luis Morales J, Hollingshead BD, Perdew GH. The aryl hydrocarbon receptor complex and the control of gene expression. Crit Rev Eukaryot Gene Expr 2008; 18:207-250.
33. Gargaro M, Scalisi G, Manni G, Mondanelli G, Grohmann U, Fallarino F. The Landscape of AhR Regulators and Coregulators to Fine-Tune AhR Functions. Int J Mol Sci 2021; 22.
34. Tarnow P, Tralau T, Luch A. Chemical activation of estrogen and aryl hydrocarbon receptor signaling pathways and their interaction in toxicology and metabolism. Expert Opin Drug Metab Toxicol 2019; 15:219-229.
35. Baba T, Mimura J, Nakamura N, Harada N, Yamamoto M, Morohashi K, Fujii-Kuriyama Y. Intrinsic function of the aryl hydrocarbon (dioxin) receptor as a key factor in female reproduction. Mol Cell Biol 2005; 25:10040-10051.
36. Gadupudi GS, Elser BA, Sandgruber FA, Li X, Gibson-Corley KN, Robertson LW. PCB126 Inhibits the Activation of AMPK-CREB Signal Transduction Required for Energy Sensing in Liver. Toxicol Sci 2018; 163:440-453.
37. Gadupudi GS, Klingelhutz AJ, Robertson LW. Diminished Phosphorylation of CREB Is a Key Event in the Dysregulation of Gluconeogenesis and Glycogenolysis in PCB126 Hepatotoxicity. Chem Res Toxicol 2016; 29:1504-1509.
38. Lai IK, Chai Y, Simmons D, Watson WH, Tan R, Haschek WM, Wang K, Wang B, Ludewig G, Robertson LW. Dietary selenium as a modulator of PCB 126-induced hepatotoxicity in male Sprague-Dawley rats. Toxicol Sci 2011; 124:202-214.
39. Cora MC, Kooistra L, Travlos G. Vaginal Cytology of the Laboratory Rat and Mouse: Review and Criteria for the Staging of the Estrous Cycle Using Stained Vaginal Smears. Toxicol Pathol 2015; 43:776-793.
40. Marcondes FK, Bianchi FJ, Tanno AP. Determination of the estrous cycle phases of rats: some helpful considerations. Braz J Biol 2002; 62:609-614.
41. Björvang RD, Gennings C, Lin PI, Hussein G, Kiviranta H, Rantakokko P, Ruokojärvi P, Lindh CH, Damdimopoulou P, Bornehag CG. Persistent organic pollutants, pre-pregnancy use of combined oral contraceptives, age, and time-to-pregnancy in the SELMA cohort. Environ Health 2020; 19:67.
42. Valvi D, Oulhote Y, Weihe P, Dalgård C, Bjerve KS, Steuerwald U, Grandjean P. Gestational diabetes and offspring birth size at elevated environmental pollutant exposures. Environ Int 2017; 107:205-215.
43. Lauritzen HB, Larose TL, Øien T, Sandanger TM, Odland J, van de Bor M, Jacobsen GW. Maternal serum levels of perfluoroalkyl substances and organochlorines and indices of fetal growth: a Scandinavian case-cohort study. Pediatr Res 2017; 81:33-42.
44. Muto T, Imano N, Nakaaki K, Takahashi H, Hano H, Wakui S, Furusato M. Estrous cyclicity and ovarian follicles in female rats after prenatal exposure to 3,3',4,4',5-pentachlorobiphenyl. Toxicol Lett 2003; 143:271-277.

45. Augustowska K, Wójtowicz A, Kajta M, Ropstad E, Gregoraszczuk EL. Polichlorinated biphenyls (PCB126 and PCB 153) action on proliferation and progesterone secretion by cultured in vitro porcine luteal cells. Exp Clin Endocrinol Diabetes 2001; 109:416-418.
46. Gregoraszczuk EL, Ptak A, Karniewska M, Ropstad E. Action of defined mixtures of PCBs, p,p'-DDT and its metabolite p,p'-DDE, on co-culture of porcine theca and granulosa cells: steroid secretion, cell proliferation and apoptosis. Reprod Toxicol 2008; 26:170-174.
47. Mlynarczuk J, Kowalik M. The effect of PCB126, 77, and 153 on the intracellular mobilization of Ca+2 in bovine granulosa and luteal cells after FSH and LH surge in vitro. Pol J Vet Sci 2013; 16:417-424.
48. Zhong T, Zhang J, Han X, Gongye X, Lyu T, Jiang M, Yu K, Meng X, Cheng D, Lyu H, Zhang T, Zhang L, et al. 3,3',4,4',5-Pentachlorobiphenyl influences mitochondrial apoptosis pathway in granulosa cells. J Cell Biochem 2019; 120:15337-15346.
49. Fan H, Su X, Yang B, Zhao A. Aryl hydrocarbon receptor and unexplained miscarriage. J Obstet Gynaecol Res 2017; 43:1029-1036.
50. Fisher JW, Campbell J, Muralidhara S, Bruckner JV, Ferguson D, Mumtaz M, Harmon B, Hedge JM, Crofton KM, Kim H, Almekinder TL. Effect of PCB 126 on hepatic metabolism of thyroxine and perturbations in the hypothalamic-pituitary-thyroid axis in the rat. Toxicol Sci 2006; 90:87-95.
51. Hoyer PB, Keating AF. Xenobiotic effects in the ovary: temporary versus permanent infertility. Expert Opin Drug Metab Toxicol 2014; 10:511-523.
52. Devillers MM, Petit F, Giton F, François CM, Juricek L, Coumoul X, Magre S, Cohen-Tannoudji J, Guigon CJ. Age-dependent vulnerability of the ovary to AhR-mediated TCDD action before puberty: Evidence from mouse models. Chemosphere 2020; 258:127361.
53. Flaws JA, Langenberg P, Babus JK, Hirshfield AN, Sharara FI. Ovarian volume and antral follicle counts as indicators of menopausal status. Menopause 2001; 8:175-180.
54. Rowlands JC, Gustafsson JA. Aryl hydrocarbon receptor-mediated signal transduction. Crit Rev Toxicol 1997; 27:109-134.
55. Shimada T, Sugie A, Shindo M, Nakajima T, Azuma E, Hashimoto M, Inoue K. Tissue-specific induction of cytochromes P450 1A1 and 1B1 by polycyclic aromatic hydrocarbons and polychlorinated biphenyls in engineered C57BL/6J mice of arylhydrocarbon receptor gene. Toxicol Appl Pharmacol 2003; 187:1-10.
56. Thompson KE, Bourguet SM, Christian PJ, Benedict JC, Sipes IG, Flaws JA, Hoyer PB. Differences between rats and mice in the involvement of the aryl hydrocarbon receptor in 4-vinylcyclohexene diepoxide-induced ovarian follicle loss. Toxicol Appl Pharmacol 2005; 203:114-123.
57. Shirota M, Mukai M, Sakurada Y, Doyama A, Inoue K, Haishima A, Akahori F, Shirota K. Effects of vertically transferred 3,3',4,4',5-pentachlorobiphenyl (PCB-126) on the reproductive development of female rats. J Reprod Dev 2006; 52:751-761.
58. Banu SK, Stanley JA, Sivakumar KK, Arosh JA, Burghardt RC. Resveratrol protects the ovary against chromium-toxicity by enhancing endogenous antioxidant enzymes and inhibiting metabolic clearance of estradiol. Toxicol Appl Pharmacol 2016; 303:65-78.
59. Stanley JA, Sivakumar KK, Nithy TK, Arosh JA, Hoyer PB, Burghardt RC, Banu SK. Postnatal exposure to chromium through mother's milk accelerates follicular atresia in

F1 offspring through increased oxidative stress and depletion of antioxidant enzymes. Free Radic Biol Med 2013; 61:179-196.
60. Sun J, Zhang X, Cao Y, Zhao Q, Bao E, Lv Y. Ovarian Toxicity in Female Rats after Oral Administration of Melamine or Melamine and Cyanuric Acid. PLoS One 2016; 11:e0149063.
61. Lim J, Luderer U. Oxidative damage increases and antioxidant gene expression decreases with aging in the mouse ovary. Biol Reprod 2010; 84:775-782.
62. Mahata P. Biomarkers for epithelial ovarian cancers. Genome Inform 2006; 17:184-193.
63. Xu X, Qin L, Tian Y, Wang M, Li G, Du Y, Chen ZJ, Li W. Family-based analysis of GGT1 and HNF1A gene polymorphisms in patients with polycystic ovary syndrome. Reprod Biomed Online 2018; 36:115-119.
64. Shen H, Robertson LW, Ludewig G. Regulatory effects of dioxin-like and non-dioxin-like PCBs and other AhR ligands on the antioxidant enzymes paraoxonase 1/2/3. Environmental Science and Pollution Research 2016; 23:2108-2118.
65. Kim K, Bloom MS, Fujimoto VY, Browne RW. Associations between PON1 enzyme activities in human ovarian follicular fluid and serum specimens. PLOS ONE 2017; 12:e0172193.
66. Liao D, Yu H, Han L, Zhong C, Ran X, Wang D, Mo L. Association of PON1 gene polymorphisms with polycystic ovarian syndrome risk: a meta-analysis of case–control studies. Journal of Endocrinological Investigation 2018; 41:1289-1300.
67. Saed GM, Ali-Fehmi R, Jiang ZL, Fletcher NM, Diamond MP, Abu-Soud HM, Munkarah AR. Myeloperoxidase serves as a redox switch that regulates apoptosis in epithelial ovarian cancer. Gynecologic Oncology 2010; 116:276-281.
68. Shimada AL, Cruz WS, Loiola RA, Drewes CC, Dörr F, Figueiredo NG, Pinto E, Farsky SH. Absorption of PCB126 by upper airways impairs G protein-coupled receptor-mediated immune response. Sci Rep 2015; 5:14917.
69. Pan X, Inouye K, Ito T, Nagai H, Takeuchi Y, Miyabara Y, Tohyama C, Nohara K. Evaluation of relative potencies of PCB126 and PCB169 for the immunotoxicities in ovalbumin (OVA)-immunized mice. Toxicology 2004; 204:51-60.
70. Quabius ES, Krupp G, Secombes CJ. Polychlorinated biphenyl 126 affects expression of genes involved in stress-immune interaction in primary cultures of rainbow trout anterior kidney cells. Environ Toxicol Chem 2005; 24:3053-3060.
71. Assou S, Anahory T, Pantesco V, Le Carrour T, Pellestor F, Klein B, Reyftmann L, Dechaud H, De Vos J, Hamamah S. The human cumulus--oocyte complex gene-expression profile. Hum Reprod 2006; 21:1705-1719.
72. Kim YH, Shin EA, Jung JH, Park JE, Koo J, Koo JI, Shim BS, Kim SH. Galbanic acid potentiates TRAIL induced apoptosis in resistant non-small cell lung cancer cells via inhibition of MDR1 and activation of caspases and DR5. Eur J Pharmacol 2019; 847:91-96.
73. Chang AS, Dale AN, Moley KH. Maternal diabetes adversely affects preovulatory oocyte maturation, development, and granulosa cell apoptosis. Endocrinology 2005; 146:2445-2453.
74. Lliberos C, Liew SH, Mansell A, Hutt KJ. The Inflammasome Contributes to Depletion of the Ovarian Reserve During Aging in Mice. Front Cell Dev Biol 2020; 8:628473.

75. Ito M, Yoshino O, Ono Y, Yamaki-Ushijima A, Tanaka T, Shima T, Orisaka M, Iwase A, Nakashima A, Saito S. Bone morphogenetic protein-2 enhances gonadotropin-independent follicular development via sphingosine kinase 1. Am J Reprod Immunol 2020:e13374.
76. da Cunha EV, Melo LRF, Sousa GB, Araújo VR, Vasconcelos GL, Silva AWB, Silva JRV. Effect of bone morphogenetic proteins 2 and 4 on survival and development of bovine secondary follicles cultured in vitro. Theriogenology 2018; 110:44-51.
77. Zhou C, Borillo J, Wu J, Torres L, Lou YH. Ovarian expression of chemokines and their receptors. J Reprod Immunol 2004; 63:1-9.
78. Price JC, Bromfield JJ, Sheldon IM. Pathogen-associated molecular patterns initiate inflammation and perturb the endocrine function of bovine granulosa cells from ovarian dominant follicles via TLR2 and TLR4 pathways. Endocrinology 2013; 154:3377-3386.
79. Hatziagelaki E, Pergialiotis V, Kannenberg JM, Trakakis E, Tsiavou A, Markgraf DF, Carstensen-Kirberg M, Pacini G, Roden M, Dimitriadis G, Herder C. Association between Biomarkers of Low-grade Inflammation and Sex Hormones in Women with Polycystic Ovary Syndrome. Exp Clin Endocrinol Diabetes 2020; 128:723-730.
80. Huang CC, Chou CH, Chen SU, Ho HN, Yang YS, Chen MJ. Increased platelet factor 4 and aberrant permeability of follicular fluid in PCOS. J Formos Med Assoc 2019; 118:249-259.
81. Uri-Belapolsky S, Shaish A, Eliyahu E, Grossman H, Levi M, Chuderland D, Ninio-Many L, Hasky N, Shashar D, Almog T, Kandel-Kfir M, Harats D, et al. Interleukin-1 deficiency prolongs ovarian lifespan in mice. Proc Natl Acad Sci U S A 2014; 111:12492-12497.
82. Huang S, Zhao P, Yang L, Chen Y, Yan J, Duan E, Qiao J. Fractalkine is expressed in the human ovary and increases progesterone biosynthesis in human luteinised granulosa cells. Reprod Biol Endocrinol 2011; 9:95.
83. Kansra V, Groves C, Gutierrez-Ramos JC, Polakiewicz RD. Phosphatidylinositol 3-kinase-dependent extracellular calcium influx is essential for CX(3)CR1-mediated activation of the mitogen-activated protein kinase cascade. J Biol Chem 2001; 276:31831-31838.
84. Liu K, Rajareddy S, Liu L, Jagarlamudi K, Boman K, Selstam G, Reddy P. Control of mammalian oocyte growth and early follicular development by the oocyte PI3 kinase pathway: new roles for an old timer. Dev Biol 2006; 299:1-11.
85. Rowley JE, Amargant F, Zhou LT, Galligos A, Simon LE, Pritchard MT, Duncan FE. Low Molecular Weight Hyaluronan Induces an Inflammatory Response in Ovarian Stromal Cells and Impairs Gamete Development In Vitro. Int J Mol Sci 2020; 21.
86. Jang YJ, Park JI, Jeong SE, Seo YM, Dam PTM, Seo YW, Choi BC, Song SJ, Chun SY, Cho MK. Regulation of interleukin-11 expression in ovulatory follicles of the rat ovary. Reprod Fertil Dev 2017; 29:2437-2445.
87. Lind PM, Eriksen EF, Lind L, Orberg J, Sahlin L. Estrogen supplementation modulates effects of the endocrine disrupting pollutant PCB126 in rat bone and uterus: diverging effects in ovariectomized and intact animals. Toxicology 2004; 199:129-136.
88. Oliveira LJ, McClellan S, Hansen PJ. Differentiation of the endometrial macrophage during pregnancy in the cow. PLoS One 2010; 5:e13213.
89. Li H, Meng YH, Shang WQ, Liu LB, Chen X, Yuan MM, Jin LP, Li MQ, Li DJ. Chemokine CCL24 promotes the growth and invasiveness of trophoblasts through ERK1/2 and PI3K signaling pathways in human early pregnancy. Reproduction 2015; 150:417-427.

90. Guerin LR, Moldenhauer LM, Prins JR, Bromfield JJ, Hayball JD, Robertson SA. Seminal fluid regulates accumulation of FOXP3+ regulatory T cells in the preimplantation mouse uterus through expanding the FOXP3+ cell pool and CCL19-mediated recruitment. Biol Reprod 2011; 85:397-408.
91. Tanikawa N, Ohtsu A, Kawahara-Miki R, Kimura K, Matsuyama S, Iwata H, Kuwayama T, Shirasuna K. Age-associated mRNA expression changes in bovine endometrial cells in vitro. Reprod Biol Endocrinol 2017; 15:63.
92. Spratte J, Princk H, Schütz F, Rom J, Zygmunt M, Fluhr H. Stimulation of chemokines in human endometrial stromal cells by tumor necrosis factor-α and interferon-γ is similar under apoptotic and non-apoptotic conditions. Arch Gynecol Obstet 2018; 297:505-512.
93. Miller JE, Monsanto SP, Ahn SH, Khalaj K, Fazleabas AT, Young SL, Lessey BA, Koti M, Tayade C. Interleukin-33 modulates inflammation in endometriosis. Sci Rep 2017; 7:17903.
94. Lawson C, Bourcier N, Al-Akoum M, Maheux R, Naud F, Akoum A. Abnormal interleukin 1 receptor types I and II gene expression in eutopic and ectopic endometrial tissues of women with endometriosis. J Reprod Immunol 2008; 77:75-84.
95. Li T, Wang J, Guo X, Yu Q, Ding S, Xu X, Peng Y, Zhu L, Zou G, Zhang X. Possible involvement of crosstalk between endometrial cells and mast cells in the development of endometriosis via CCL8/CCR1. Biomed Pharmacother 2020; 129:110476.
96. Su Y, Guo S, Liu C, Li N, Zhang S, Ding Y, Chen X, He J, Liu X, Wang Y, Gao R. Endometrial pyruvate kinase M2 is essential for decidualization during early pregnancy. J Endocrinol 2020; 245:357-368.
97. Laghi F, Di Roberto PF, Panici PB, Margariti PA, Scribano D, Cudillo L, Villani L, Bizzi B. Coagulation disorders in patients with tumors of the uterus. Tumori 1983; 69:349-353.
98. Raliou M, Dembélé D, Düvel A, Bolifraud P, Aubert J, Mary-Huard T, Rocha D, Piumi F, Mockly S, Heppelmann M, Dieuzy-Labaye I, Zieger P, et al. Subclinical endometritis in dairy cattle is associated with distinct mRNA expression patterns in blood and endometrium. PLoS One 2019; 14:e0220244.
99. Meng YH, Zhou WJ, Jin LP, Liu LB, Chang KK, Mei J, Li H, Wang J, Li DJ, Li MQ. RANKL-mediated harmonious dialogue between fetus and mother guarantees smooth gestation by inducing decidual M2 macrophage polarization. Cell Death Dis 2017; 8:e3105.
100. Han J, Gu MJ, Yoo I, Choi Y, Jang H, Kim M, Yun CH, Ka H. Analysis of cysteine-X-cysteine motif chemokine ligands 9, 10, and 11, their receptor CXCR3, and their possible role on the recruitment of immune cells at the maternal-conceptus interface in pigs. Biol Reprod 2017; 97:69-80.
101. Chaturvedi V, Ertelt JM, Jiang TT, Kinder JM, Xin L, Owens KJ, Jones HN, Way SS. CXCR3 blockade protects against Listeria monocytogenes infection-induced fetal wastage. J Clin Invest 2015; 125:1713-1725.
102. Chen M, Zhou Y, Xu H, Hill C, Ewing RM, He D, Zhang X, Wang Y. Bioinformatic analysis reveals the importance of epithelial-mesenchymal transition in the development of endometriosis. Sci Rep 2020; 10:8442.
103. Złotkowska A, Andronowska A. Chemokines as the modulators of endometrial epithelial cells remodelling. Sci Rep 2019; 9:12968.

104. Young VJ, Brown JK, Maybin J, Saunders PT, Duncan WC, Horne AW. Transforming growth factor-β induced Warburg-like metabolic reprogramming may underpin the development of peritoneal endometriosis. J Clin Endocrinol Metab 2014; 99:3450-3459.
105. Kusakabe K, Kiso Y, Hondo E, Takeshita A, Kato K, Okada T, Shibata MA, Otsuki Y. Spontaneous endometrial hyperplasia in the uteri of IL-2 receptor beta-chain transgenic mice. J Reprod Dev 2009; 55:273-277.
106. Rier S, Foster WG. Environmental dioxins and endometriosis. Semin Reprod Med 2003; 21:145-154.

Figure Legends:

Figure 1. Impact of PCB126 exposure in WT and AHR$^{-/-}$ rats on body and reproductive organ weights. At the end of the dosing period, body, ovarian and uterine weights were recorded. Bars are presented as mean (A) body weight (g), (B) relative ovarian weight and (C) relative uterine weight ± SEM. * indicates statistical difference between indicated treatments; $P < 0.05$.

Figure 2. Endocrine impacts of PCB126 exposure and AHR deficiency. Serum collected at the end of the dosing period was analyzed for (A) FSH, (B) LH, (C) progesterone, (D) Testosterone, (E) 17β-estradiol, or (F) AMH. Bars are presented as mean hormone level ± SEM. * indicates statistical difference between indicated treatments; $P < 0.05$.

Figure 3. Effect of PCB126 exposure and AHR deficiency on ovarian follicle number. Ovarian follicle counts were performed on blinded hematoxylin and eosin-stained sections and follicles were classified as (A) primordial, (B) primary, (C) secondary, (D) antral or (E) corpora lutea. Follicle numbers are presented as mean ± SEM. * indicates statistical difference between indicated treatments; $P < 0.05$.

Figure 4. Effect of PCB126 exposure and AHR deficiency on uterine area and gland number. Fixed uteri were analyzed for (A) uterine gland number, (B) uterine area and (C) uterine glands/area. Bars represent mean ± SEM. * indicates statistical difference between indicated treatments; $P < 0.05$.

Figure 5. Effect of PCB126 and AHR deficiency on estrogen receptor protein abundance. Assessment of (A) estrogen receptor alpha, and (B) estrogen receptor beta protein abundance in the uterine stroma, glandular epithelium (GE) and luminal epithelium (LE) was performed using immunohistochemistry. Immunofluorescent signal quantification (pixels) was assessed using Image J software in a blinded fashion. Means ± SEM of those assessments are presented per experimental group and per uterine compartment. * indicates statistical difference between indicated treatments; $P < 0.05$.

Table 1. Impact of PCB126 exposure on ovarian abundance of mRNA encoding chemical biotransformation genes in WT rats.

Gene name	Fold Change
Cyp1a1	152.9
Adh4	112.9
Aoc1	64.3
Cyp27b1	59.4
Marcks	46.2
Cyp2b3	43.1
Cyp3a23/3a1	43.1
Cyp1a2	36.3
Pon1	35.6
Gckr	29.2
Ces2c	29.1
Gpx5	27.5
Gstm3	27.0
Mpo	21.7
Cyp2c13	20.7
Cyp1b1	18.1
Alox15	17.2
Adh1	16
Alox5	14.8
Cyp2c7	14.8
Lpo	14.3
Nqo1	10.3
Cyp2c6v1	9.8
Gpx2	7.6
Cyp2e1	7.2
Hk2	6.9
RGDC	6.7
Aldh1a1	6.7
Nos2	6.2
Ahr	6.2
Chst1	6.2
Pklr	5.9
Hsd17b2	5.7
Hsd17b3	5.1
Fbp1	5.1
Alad	5.0
Arnt	5.0
Cyp19a1	4.4

Srd5a1	4.3
Hsd17b1	3.2
Gstp1	2.9
Xdh	2.8
Mthfr	2.5
Cyp17a1	2.3
Ggt1	-3.6
Gpx1	-6.0

Data indicate the relative difference (fold-change) in mRNA abundance of ovarian genes involved in chemical biotransformation which are abbreviated and listed in the left column. The fold-change is listed in the right column and represents difference between WT_O and WT_PCB rats with positive values indicating greater abundance in WT_O rats and negative values indicating greater abundance in WT_PCB rats.

Table 2. Impact of AHR deficiency on ovarian abundance of mRNA encoding chemical biotransformation genes in rats.

Gene name	Fold Change
Adh4	77.7
Aoc1	44.1
Cyp2b3	32.4
Marcks	32.4
Cyp27b1	31.9
Cyp3a23/3a1	27.5
Cyp1a2	25.3
Pon1	25.0
Gckr	16.1
Ces2c	16.1
Cyp2b15	15.0
Cyp2c13	14.9
Mpo	13.0
Lpo	11.9
Adh1	11.5
Cyp2c7	10.1
Nqo1	5.7
Gpx2	5.7
Fbp1	4.5
Hsd17b2	4.5
Pklr	4.3
Aldh1a1	4.2
Hk2	4.0
Chst1	3.9
Hsd17b3	3.4
Arnt	3.2
Alad	3.0
Ahr	3.0
Gad1	3.0
Cyp19a1	2.8
Gpx1	-3.8

Data indicate the relative difference (fold-change) in mRNA abundance of ovarian genes involved in chemical biotransformation which are abbreviated and listed in the left column. The fold-change is listed in the right column and represents difference between $WT^{-/-}$_O and $AHR^{-/-}$_O rats.

Table 3. Impact of PCB126 exposure on ovarian abundance of mRNA encoding inflammation genes in WT rats.

Gene name	Fold Change
Tnfrsf11b	3.7
Il6st	2.9
Ccr1	2.8
Bmp2	2.7
Csf1	2.7
Il33	2.5
Cx3cr1	2.4
Pf4	2.2
Tnfsf10	2.1
Il1r1	2.1

Data indicate the relative difference (fold-change) in mRNA abundance of ovarian genes involved in inflammation which are abbreviated and listed in the left column. The fold-change is listed in the right column and represents difference between WT_O and WT_PCB rats.

Table 4. Impact of PCB126 exposure on ovarian abundance of mRNA encoding inflammation genes in AHR$^{-/-}$ rats.

Gene name	Fold Change
Ccl11	-2.2
Ccl22	-2.0
Il11	-2.0

Data indicate the relative difference (fold-change) in mRNA abundance of ovarian genes involved in inflammation which are abbreviated and listed in the left column. The fold-change is listed in the right column and represents difference between AHR$^{-/-}$_O and AHR$^{-/-}$_PCB rats.

Table 5. Impact of AHR deficiency on ovarian abundance of mRNA encoding inflammation genes in rats.

Gene name	Fold Change
Cxcl10	-4.0
Il17b	-3.4
Cxcl2	-2.8

Data indicate the relative difference (fold-change) in mRNA abundance of ovarian genes involved in inflammation which are abbreviated and listed in the left column. The fold-change is listed in the right column and represents difference between WT_O and AHR$^{-/-}$_O rats. Negative values indicate reduced abundance in AHR$^{-/-}$_O rats.

Table 6. Impact of PCB126 exposure on uterine abundance of mRNA encoding inflammation genes in WT rats.

Gene name	Fold Regulation
Ccl24	12.9
Il33	8.6
Cx3cr1	5.4
Pf4	4.8
Bmp2	4.8
Ccr1	3.8
Tnfrsf11b	3.4
Ccl19	3.3
Ccl5	2.8
Cxcl12	2.6
Il1r1	2.6
Cxcr5	2.3
Ldha	-2.5

Data indicate the relative difference (fold-change) in mRNA abundance of uterine genes involved in inflammation which are abbreviated and listed in the left column. The fold-change is listed in the right column and represents difference between WT_O and WT_PCB rats.

Table 7. Impact of AHR deficiency on uterine abundance of mRNA encoding inflammation genes in rats.

Gene name	Fold Regulation
Il2rb	3.0

Data indicate the relative difference (fold-change) in mRNA abundance of uterine genes involved in inflammation which are abbreviated and listed in the left column. The fold-change is listed in the right column indicates greater abundance of *Il2rb* in $AHR^{-/-}$_O compared to WT_O rats.

CRediT author statement

Violet Klenov, Susanne Flor, Shanthi Ganesan, Malavika Adur, Nazmin Eti, Kursheed Iqbal: Rat model development, Animal exposures and all Laboratory analysis. **Violet Klenov**: Original paper draft preparation. **Michael Soares, Jason Ross, Gabriele Ludewig, Larry Robertson, Aileen Keating:** Conceptualization; Supervision; Writing - Reviewing and Editing. **All authors**: manuscript reviewing and editing.

Declaration of interests

☒ The authors declare that they have no known competing financial interests or personal relationships that could have appeared to influence the work reported in this paper.

☐The authors declare the following financial interests/personal relationships which may be considered as potential competing interests:

Highlights:

PCB126 reduced body and ovarian weight and depleted follicles in wildtype rats.

PCB126 exposure disrupted the endocrine environment in wildtype rats.

PCB126 exposure altered chemical metabolism and inflammation mRNA level.

Lack of AHR in rats was protective against many PCB126 alterations.

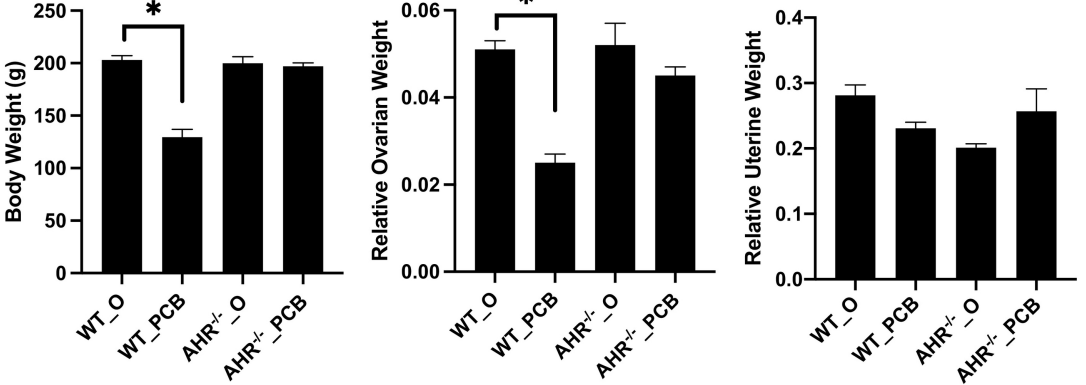
Body Weight (g)
250
200
150
100
50
0
*
WT_O
WT_PCB
AHR-/- _O
AHR-/- _PCB
Relative Ovarian Weight
0.06
0.04
0.02
0.00
*
WT_O
WT_PCB
AHR-/- _O
AHR-/- _PCB
Relative Uterine Weight
0.4
0.3
0.2
0.1
0.0
WT_O
WT_PCB
AHR-/- _O
AHR-/- _PCB

Figure 1

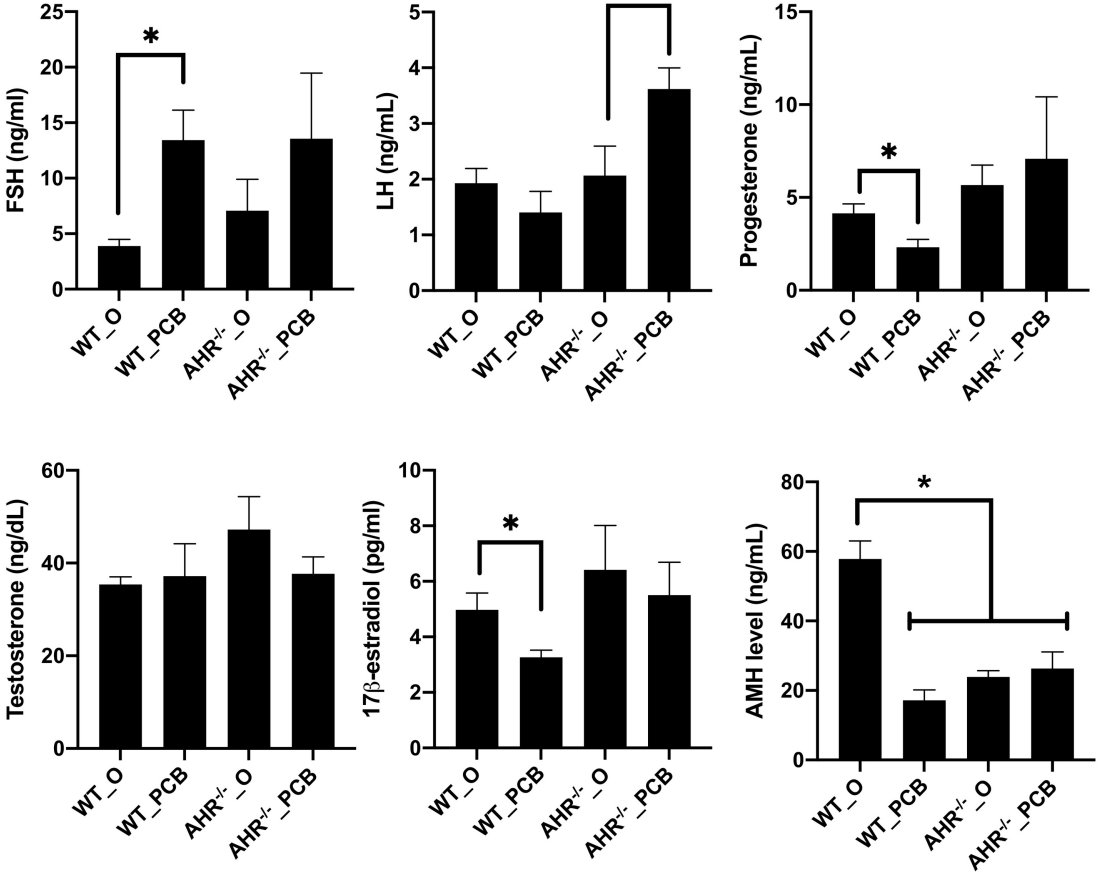
FSH (ng/ml)
LH (ng/mL)
Progesterone (ng/mL)
Testosterone (ng/dL)
17β-estradiol (pg/ml)
AMH level (ng/mL)
WT_O
WT_PCB
AHR-/- _O
AHR-/- _PCB
*

Figure 2

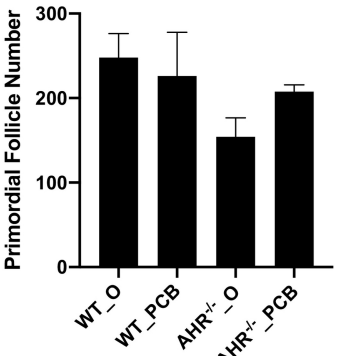
Primordial Follicle Number
300
200
100
0
WT_O
WT_PCB
AHR-/- _O
AHR-/- _PCB

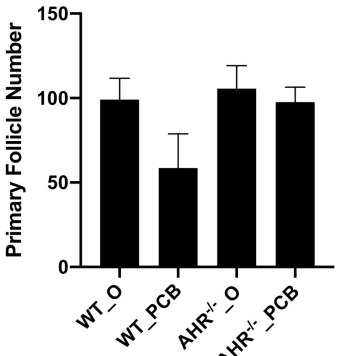
Primary Follicle Number
150
100
50
0
WT_O
WT_PCB
AHR+/- _O
AHR-/- _PCB

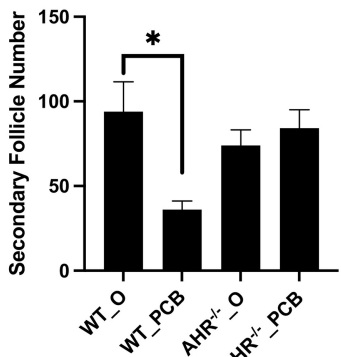
Secondary Follicle Number
150
100
50
0
*
WT_O
WT_PCB
AHR-/- _O
AHR-/- _PCB

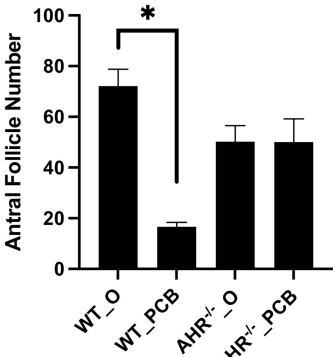
Antral Follicle Number
100
80
60
40
20
0
*
WT_O
WT_PCB
AHR-/- _O
AHR-/- _PCB

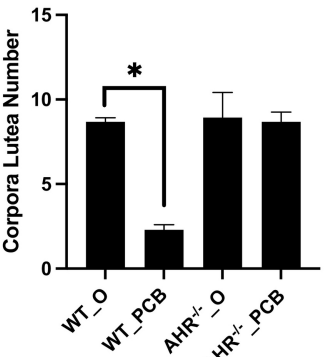
Corpora Lutea Number
15
10
5
0
*
WT_O
WT_PCB
AHR-/- _O
AHR-/- _PCB

Figure 3

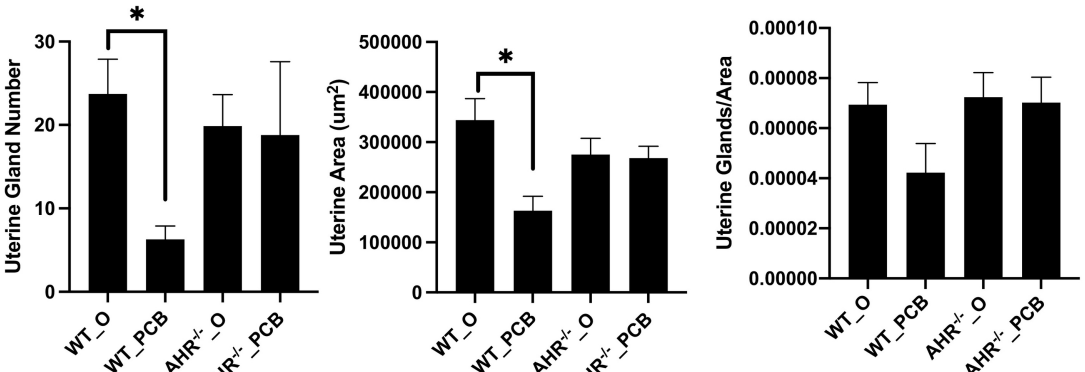
Uterine Gland Number
30
20
10
0
*
WT_O
WT_PCB
AHR-/- _O
AHR-/- _PCB
Uterine Area (um2)
500000
400000
300000
200000
100000
0
*
WT_O
WT_PCB
AHR-/- _O
AHR-/- _PCB
Uterine Glands/Area
0.00010
0.00008
0.00006
0.00004
0.00002
0.00000
WT_O
WT_PCB
AHR-/- _O
AHR-/- _PCB

Figure 4

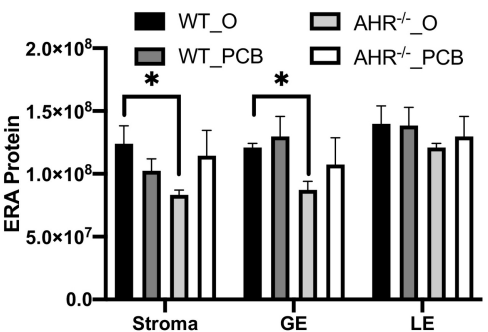
WT_O
WT_PCB
AHR-/-_O
AHR-/-_PCB
2.0×10^8
1.5×10^8
1.0×10^8
5.0×10^7
0.0
ERA Protein
*
*
Stroma
GE
LE

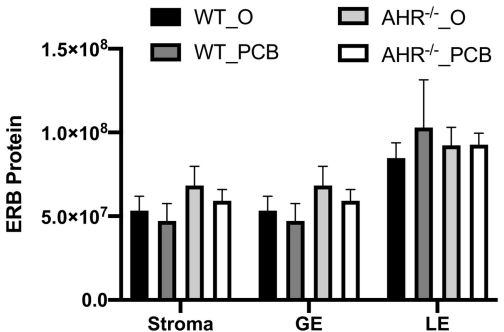
WT_O
WT_PCB
AHR-/-_O
AHR-/-_PCB
1.5×10^8
1.0×10^8
5.0×10^7
0.0
ERB Protein
Stroma
GE
LE

Figure 5

PCB126 effects

Uterine weight
Luteinizing hormone
Testosterone
Uterine gland/area
Uterine ERA and ERB protein level

Increased
Follicle stimulating hormone
Ovarian chemical biotransformation mRNAs (44)
Ovarian inflammation mRNAs (10)
Uterine inflammation mRNAs (12)

Decreased
Body weight
Ovarian weight
17β-estradiol
Progesterone
Anti-Müllerian hormone
Follicle and Corpora lutea number
Uterine glands
Uterine area
Ovarian chemical biotransformation mRNAs (2)
Uterine inflammation mRNAs (1)

No Effect
Body weight
Ovarian weight
Uterine weight
Follicle stimulating hormone
Testosterone
17β-estradiol
Progesterone
Anti-müllerian hormone
Follicle and corpora lutea number
Uterine glands
Uterine area
Uterine gland/area
Uterine ERA and ERB protein level
Ovarian chemical biotransformation mRNAs
Uterine inflammation mRNAs

Increased
Luteinizing hormone

Decreased
Ovarian inflammation mRNAs (3)

AHR deficiency effects

No Effect
Body weight
Ovarian weight
Uterine weight
Follicle stimulating hormone
Luteinizing hormone
Testosterone
17β-estradiol
Progesterone
Follicle and corpora lutea number
Uterine glands
Uterine area
Uterine gland/area
Uterine ERB protein level

Increased
Ovarian chemical biotransformation mRNAs (30)
Uterine inflammation mRNA (*Il2rb*)

Decreased
Anti-müllerian hormone
Uterine stroma and GE ERA protein level
Ovarian chemical biotransformation mRNA (*Gpx1*)
Ovarian inflammation mRNAs (3)

Figure 6